Journal of Thermal Analysis and Calorimetry, Vol. 65 (2001) 281–293

SYNTHESIS AND THERMOANALYTICAL INVESTIGATION OF AN AMORPHOUS PRASEODYMIUM CITRATE*

M. Popa and M. Kakihana

Materials and Structures Laboratory, Tokyo Institute of Technology, Nagatsuta 4259, Midori-ku, Yokohama 226-8503, Japan

(Received January 22, 2001)

Abstract

The present research describes the synthesis of the citrate of Pr by the amorphous citrate method and the study of the thermal decomposition of the complex in air, nitrogen and oxygen, in order to identify the final compounds and the intermediates obtained during the decomposition. A special study was dedicated to the thermal decomposition of the Pr-carbonate octahydrate used in the synthesis as starting material. The thermal decomposition of the lanthanide citrate was investigated mainly by thermogravimetry, differential thermal analysis, X-ray diffraction and infrared spectroscopy. The results showed that the complex decomposes to $PrO_{1.83}$ with formation of an intermediate oxycarbonate compound in air or directly to the oxide in oxygen; in nitrogen atmosphere, amorphous products were obtained after thermal decomposition.

Keywords: amorphous citrate method, praseodymium citrate, praseodymium oxide, thermal decomposition

Introduction

Characterization of the thermal decomposition process provides useful information on understanding the conditions required to produce solid materials with specific properties. The formation of the metal oxides from inorganic precursors is extensively used to obtain materials with technological interest. Lanthanide complexes are useful in catalysis and adsorption processes as they can be employed for the synthesis of solids with reactive surfaces, therefore the thermal decomposition of acetates, oxalates, caproates, malonates, etc., the nature and the stability of the intermediates and the stoichiometry of the final compounds have received increasing interest. The interest in rare earth oxides has been promoted by their potential applications in analytical chemistry and inorganic and coordination chemistry [1–3]. In the literature, there are disagreements on the decomposition temperature and products structure, stability of

---

* Presented at the Solid State Chemistry 2000 Conference in September 2000, Prague, Czech Republic

1418–2874/2001/ $ 5.00

Akadémiai Kiadó, Budapest
Kluwer Academic Publishers, Dordrecht

the intermediates and the final oxides stoichiometry of rare-earth complexes, therefore a detailed study of the phases present in these systems at various temperatures is of very practical interest.

The oxidizability of praseodymium makes the complexes of this rare earth element the less stable in the group of rare-earth elements complexes, even when heated in vacuum [4, 5]. For Pr(IV) only few compounds are known, the most common being the black non-stoichiometric oxide formed on heating Pr(III) salts or Pr_2O_3 in air. The oxide system which is often formulated as Pr_6O_{11} is actually very complicated [6]. Pr_6O_{11} dissolves in acids to give aqueous Pr(III) and liberates oxygen, chlorine and so on, depending on the acid used. Pr(IV) is a very powerful oxidizing agent, the Pr(IV)/Pr(III) couple being estimated as +2.9 V. This potential is such that Pr(IV) would oxidize water itself, therefore its non-existence in solution is not surprising [7]. Pr oxides comprise different stoichiometries and structures: the hexagonal Pr_2O_3, the fluorite-type PrO_2 and other intermediate oxygen-deficient modifications of the fluorite-type PrO_x, where $x<2$ [5]. The decomposition of praseodymium acetates [4, 8], oxalates [4, 8–10], malonates [2, 11], caproates [12] or hydrated Pr benzene-1,4-dioxyacetate in air or different atmospheres [13, 14] results in the formation of the anhydrous Pr-carbonate. Our present research is related to the synthesis and characterization of a praseodymium citrate (Pr-CA, where CA is citric acid: $C_6H_7O_8$) complex with Pr-carbonate octahydrate as source of Pr, its final decomposition products and to suggest a mechanism of the thermal decomposition of the complex.

We applied for synthesis the amorphous citrate route for the synthesis, which involves a liquid-mixing technique in concentrated citrate solutions with addition of a minimum quantity of water and using as starting material carbonates. The amorphous citrate method is commonly chosen for the preparation of oxide materials because of its versatility and simplicity [15], being a simple modified citrate gel method for the synthesis of many systems, which involves the elimination of the step of pH control for obtaining a citrate gel. Following our research concerning the preparation of $PrBa_2Cu_4O_8$ system applying the amorphous citrate method [16, 17], this paper deals with the study of the thermal decomposition of the citrate of Pr under the conditions used to generate stable, homogeneous, ultrafine powders in the system $Pr(Ca)Ba_2Cu_4O_8$. The amorphous Pr-CA complex is meant as a precursor for the preparation of the powders in the $PrBa_2Cu_4O_8$ system. A survey of the literature shows that there are no data reported on Pr-CA based compounds, therefore, this research is focused on the decomposition, the nature and stability of the intermediates, the influence of the composition of the gas atmosphere i.e. nitrogen (N_2), oxygen (O_2) and air on the chemical composition of the generated compounds of Pr.

Experimental

Preparation method

A typical flow chart of the synthesis of Pr-CA complex is shown in Fig. 1. The metal carbonate $Pr_2(CO_3)_3{\cdot}8H_2O$ of high purity >99% provided by Kanto Chemicals Japan,

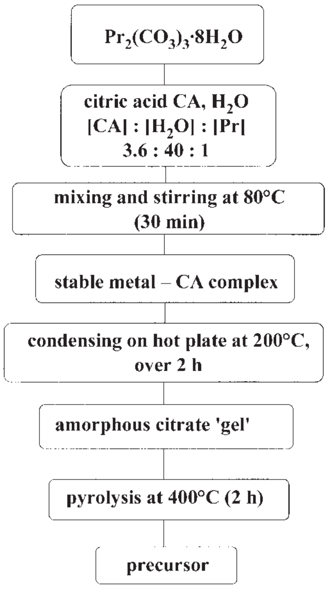

Fig. 1 Flow chart of the amorphous citrate procedure used to prepare Pr-CA complex

was used as source for Pr and citric acid (CA) and deionized pure water were used as other chemicals required for the synthesis. The metal carbonate was dissolved in water and added to the aqueous solution of CA, using the molar ratios of [CA]:[H_2O]:[Pr] of 3.6:40:1. The mixture was magnetically stirred at 80–90°C for at least 30 min, in order to obtain in the solution the stable metal-CA complex. A green and clear solution was obtained. The solution was stirred and heated at 200°C until it became a brown sticky gel; the temperature was slowly increased to 400°C over 2 h to fully evaporate highly combustible species in the gel and to burn down most of the organic constituents, charring. The resulting material had the appearance of a dark brown ash which was slightly ground into a powder by a Teflon rod. The resulting material had the appearance of a dark brown ash which was slightly ground into a powder by a Teflon rod. The as-obtained powder is referred to as the ‘precursor’ hereafter and characterized at different stages.

Characterization

The obtained material as well as the initial praseodymium carbonate were characterized by thermogravimetry (TG) and differential thermal analysis (DTA), X-ray diffraction (XRD) and infrared (IR) spectroscopy.

Simultaneous TG/DTA measurements were carried out up to 1000°C in air and in flowing oxygen and nitrogen at 1 atm and 0.25 L min^{-1}, with Al_2O_3 as reference, in a Derivatograph Type-2020, MAC Science, Japan with a heating rate of 2°C min^{-1}. Each measurement used about 5 mg of powdered sample placed in an Al_2O_3 crucible of (d×h) of (5.2×5.1) mm. Phases purities and crystal structure of the obtained materials, both from left-overs from the TG experiments and powders treated separately in the same conditions, were determined by X-ray diffraction. The XRD patterns were recorded with a standard equipment Model MXP-3VA MAC Science, Tokyo-Japan diffractometer equipped with a graphite monochromatized using CuK_{α} radiation (λ=1.5405 Å) operating at 40 mA and 40 kV, with a scanning rate of 0.4^{0} s^{-1} in the (2θ) range from 5 to 70°.

IR spectra were obtained at a resolution of 2 cm^{-1}, over the frequency range from 4000 to 370 cm^{-1}, using a model Perkin Elmer spectrophotometer. The spectra were taken from thin (~20 mg cm^{-2}) KBr pellets containing approximately 1% mass sample. Pellets were prepared by compacting an intimate mixture obtained by grinding 1 mg of substance in 100 mg KBr.

Results and discussion

A highly viscous gel was obtained by boiling the concentrate citrate solution. The synthesis method is an easy way of obtaining the Pr-CA complex. It involves no rigorous chemical procedure such as careful aging of gel or fine control of pH usually required for sol–gel methods. Basically it has two major steps consisting of the formation of the metal-citrate gel in water without aging and pH adjustment and the subsequent decomposition of the gel to obtain the powder precursor after boiling it at moderate temperature. The method yields very fine and homogeneous particles. The amorphous citrate method, or so-called the non-polymerizable route, involves the formation of weak hydrogen-bonded-like associates, in a no-rigid polymer network [15, 18]. From the concentrated metal complex solution, associates are formed which are weakly interconnected by Van der Waals or hydrogen bonding. Among many alpha-hydroxycarboxylic acids, citric acid is the most efficient ligand due to its possibility to act as a potential multidentate ligand, i.e. three carboxylic acid and one alcoholic group involved in one molecule of citric acid can coordinate to metal ions in a variety of ways. The alcoholic carbons in CA play an important role to stabilize such a metal complex, since the ($-C-O^{-}$) group has a very strong affinity to metal ions resulting in the formation of a stable chelate complex.

The ash of the gel obtained after charring was an amorphous material. During charring, spontaneous combustion can occur easily raising the sample temperature and generating the crystallization. The combustion is difficult to control and causes a highly non-uniform temperature profile on the sample. In our case the sample did not experience spontaneous combustion and became an amorphous powder after charring, since no peaks were observed on the X-ray pattern.

Considering that for the hydrated Pr-carbonate different possible mechanisms of thermal decomposition have been suggested [19–28], in order to analyze the thermal decomposition of the Pr-CA complex, we also performed studies of the starting carbonate used in our synthesis, as source of Pr. Crystallographic data on the octahydrated carbonate of Pr, determined by Raman spectroscopy and XRD, correspond

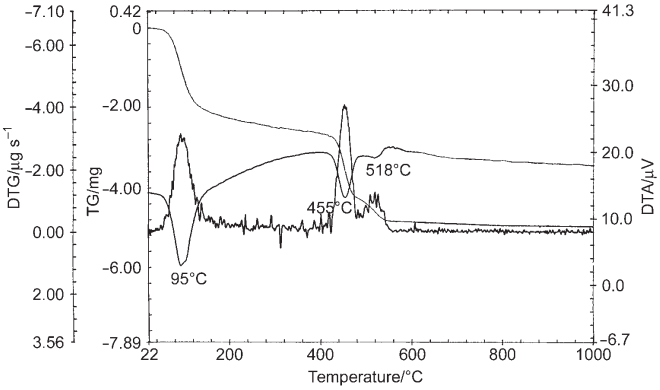

Fig. 2 The DTA/TG/DTG curves for $Pr_2(CO_3)\cdot 8H_2O$ at heating rate of 2°C min^{-1}

to an orthorhombic compound with the space group D_{2h} [19–21, 29] and to the JCPDS card file 31-1143. Figure 2 presents the thermoanalytical TG/DTA data of the $Pr_2(CO_3)_3\cdot 8H_2O$. DTA curve shows peaks in correspondence with the mass losses observed in the TG curve. Pr carbonate decomposes in three steps, corresponding to three endothermic events occurring at 95, 455 and 518°C, each step being accompanied by a mass loss. The initial mass loss observed in the TG curve is attributed to the loss of water of crystallization, the experimental mass loss of 24.36% is in good agreement with the calculated theoretical value of 23.76%. The second mass loss is due to the decomposition of the anhydrous carbonate to the $Pr_2O_2CO_3$ and in this case the experimental and theoretical values of the mass losses are 14.45 and 14.52%. The third mass loss is due to the decomposition of the intermediate compound $Pr_2O_2CO_3$ to the corresponding oxide, and the experimental and theoretical mass losses are 6.46 and 5.52%, respectively. The results are in good agreement with the X-ray diffraction data, indicating the formation of $Pr_2O_2CO_3$ (JCPDS 25-696), which finally decomposes to the corresponding oxide $PrO_{1.83}$ (JCPDS 6-329). The X-ray diffraction data taken from the product obtained from the decomposition step at 1000°C, showed that all the initial carbonate was decomposed to $PrO_{1.83}$.

The suggested reactions occurring during the thermal decomposition of the Pr carbonate are summarized below, according to the experimental and theoretical mass losses observed in the TG curves.

$$Pr_2(CO_3)_3\cdot 8H_2O \rightarrow Pr_2(CO_3)_3+8H_2O \tag{1}$$

$$Pr_2(CO_3)_3 \rightarrow Pr_2O_2CO_3+2CO_2 \tag{2}$$

$$Pr_2O_2CO_3 \xrightarrow{O_2} 2PrO_{1.83}+CO_2 \tag{3}$$

According to the TG/DTA and XRD studies we suggest the following mechanism for the thermal decomposition in air of the octahydrated Pr-carbonate used in our synthesis:

$$Pr_2(CO_3)_3\cdot 8H_2O \rightarrow Pr_2(CO_3)_3 \rightarrow Pr_2O_2CO_3 \rightarrow PrO_{1.833} \tag{4}$$

Figure 3 shows the thermoanalytical TG/DTA data in air of the Pr-citrate complex. As it can be noticed on the curves, the complex decomposes on heating accom-

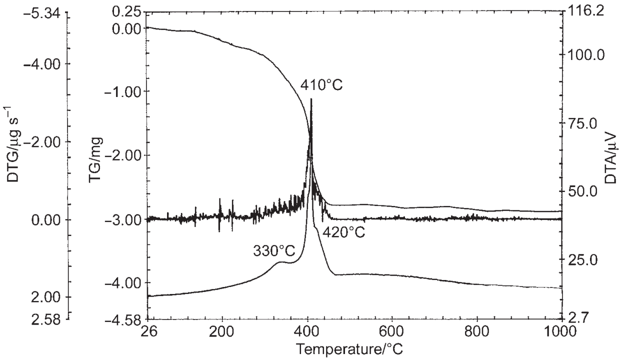

Fig. 3 The DTA/TG/DTG curves for Pr-CA complex in air at heating rate of 2°C min^{-1}

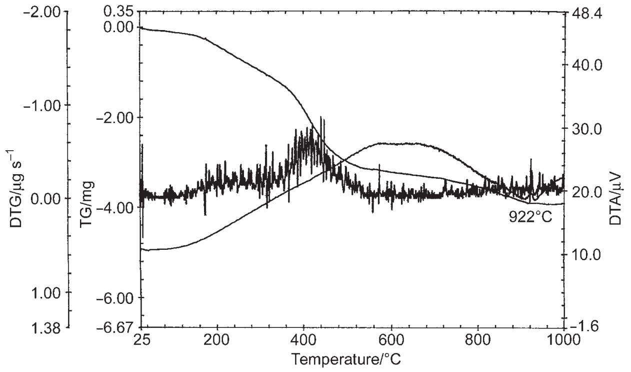

Fig. 4 The DTA/TG/DTG curves for Pr-CA complex in a dynamic 0.25 L min^{-1} of nitrogen, at heating rate of 2°C min^{-1}

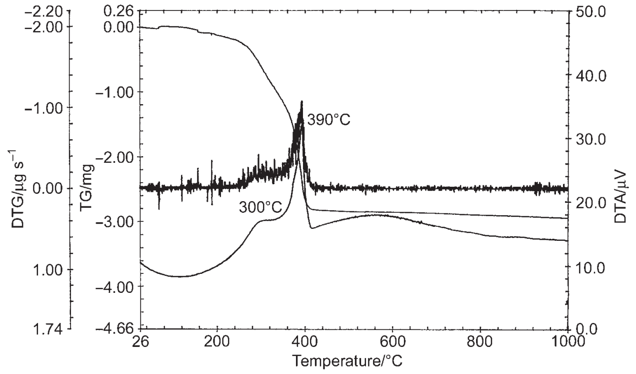

Fig. 5 The DTA/TG/DTG curves for Pr-CA complex in a dynamic 0.25 L min^{-1} of oxygen, at heating rate of 2°C min^{-1}

panied by an exothermic effect with maximum at ~410°C. DTA curve shows the presence of two other minor exothermic effects or kinds of the main exothermic peak. The exothermic effects are due to the oxidation of the organic ligands and escape of carbon and CO. As it clearly appears on the TG curve it is difficult to estimate the processes of decomposition, as many bendings of the curve can be observed but not a clear plateau.

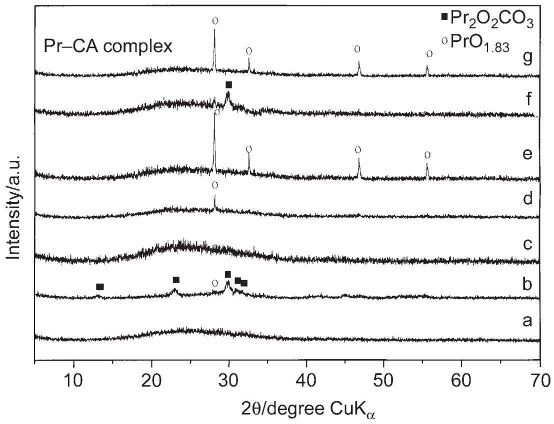

Fig. 6 The XRD results of the powder of Pr-CA complex; a – raw material and of the Pr-CA complex solid decomposition products obtained by heat treatment at 450°C for 1 h; b – in air; c – in nitrogen; d – in oxygen and obtained by heat treatment at 1000°C for 1 h; e – in air; f – in nitrogen and g – in oxygen

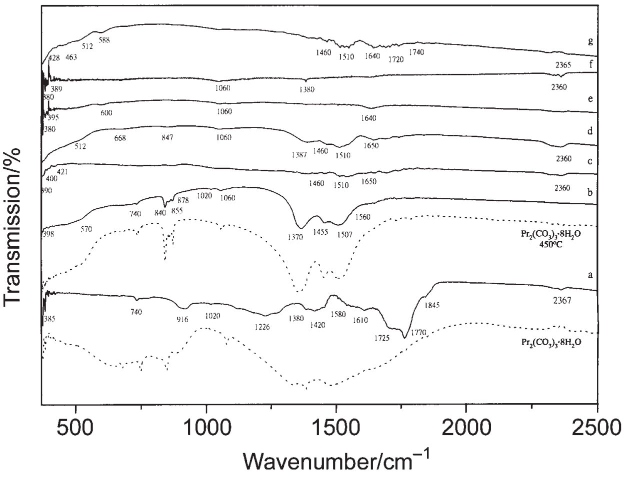

Fig. 7 The IR spectra results from KBr supported samples of Pr-CA complex; a – raw and its solid decomposition products obtained by calcining for 1 h at 450°C; b – in air; c – in nitrogen; d – in oxygen and obtained by heat treatment at 1000°C for 1 h; e – in air; f – in nitrogen and g – in oxygen. With dotted line results are represented for comparison the IR spectra from KBr supported samples of $Pr_2(CO_3)_3 \cdot 8H_2O$ and its solid decomposition product obtained in air at 450°C

DTA/TG/DTG curves of the Pr-citrate decomposition in nitrogen and oxygen are shown in Figs 4 and 5. The DTA/TG/DTG curves of the Pr-citrate decomposition in air, oxygen and nitrogen show that the decomposition depends on the ambient atmosphere.

XRD and IR results of the raw complex, the intermediate compounds and final products obtained during the decomposition in air, oxygen and nitrogen, are shown in Figs 6 and 7. The structure obtained by XRD for the Pr-CA complex is that of an amorphous compound. Different intermediates were detected as stable phases during the decomposition of the citrate, depending on the atmosphere used. Pr-CA complex decomposes into a mixture of $Pr_2O_2CO_3$ (JCPDS 25-696) and $PrO_{1.83}$ (JCPDS 6-329) in air at 450°C, while a quite amorphous compound was noticed in the case of the citrate decomposition in N_2. On the XRD pattern, only a peak corresponding to the $Pr_2O_2CO_3$ (JCPDS 25-696) could be registered. $PrO_{1.83}$ was found as an intermediate, without traces of oxycarbonate in the case of the decomposition in oxygen atmosphere. Different compounds were obtained as final products after decomposition at 1000°C. $PrO_{1.83}$ was obtained in the case of the decomposition in air and in oxygen atmosphere while an amorphous phase was obtained in the case of the nitrogen atmosphere. Compared to the Pr-carbonate which decompose to $PrO_{1.83}$ through $Pr_2O_2CO_3$ as intermediate, the Pr-CA complex, according to the DTA/TG curve decomposes to $PrO_{1.83}$ with a strong exothermic effect.

IR spectra of the Pr-citrate complex displayed absorptions at 3420 and 1640 cm^{-1} due to ν_{OH} and δ_{HOH} vibrations of water molecules. Absorption bands due to carboxyl ions (COO^-) are found ~1380 cm^{-1} – the symmetrical stretching band – and near 1580 cm^{-1} – the asymmetrical stretching band. The most intense absorptions in the spectrum of the raw citrate complex at ~1725 and ~1770 cm^{-1} and the band at 1845 cm^{-1} are due to the carbonyl stretching mode in the –COOH carboxylic acid groups of citric acid [30, 31]. For comparison, it can be observed the IR spectra of the Pr-carbonate octahydrate represented with dotted line. IR spectra displayed absorption between 1480–1380 cm^{-1} due to the (OCO) group frequency, at 1480 cm^{-1} the asymmetric vibrations frequency $\nu_{as}(COO^-)$ and at 1380 cm^{-1} the symmetric vibrations frequency $\nu_s(COO^-)$ respectively, as well as at 660, 680 and 720 cm^{-1} due to the $\delta(COO)^-$ deformation vibrations. Pr-CA complex shows coordinations which are found in the majority of carbonato-complexes, with the mention that the splitting of the vibrations is more pronounced compared to the Pr-carbonate octahydrate, because of the character more covalent of the bonds, observation which agrees with the literature data [32], however, it is difficult to determine precisely the IR bands in the case of Pr-CA complex in the region of the asymmetrical and symmetrical bands of COO^- carboxyl ions, the IR bands are not well defined. IR spectrum of the calcination product of Pr-CA complex at 450°C shows the formation of oxycarbonate band structure with characteristic peaks at 740, 840, 855, 878, 1060, 1370, 1455, 1507 and 1560 cm^{-1} [4, 5, 19, 32, 33]. According to the literature reported data [19, 31] the band frequencies help deciding the bidentate or unidentate complex formed in the process. The complexation occurred with the bridging of polydentate citrate ligand establishing the chelate bonding in the metal-CA complex formed during reaction.

Splitting of the vibrations of the solid products after treatment at 450°C shows the IR bands characteristic of an unidentate complex formed as intermediate in the process of Pr-CA complex decomposition. XRD pattern of the powder at 450°C in air indicates that $Pr_2O_2CO_3$ (JCPDS No. 25-696) is the detectable phase. All features in our case are characteristic of a unidentate carbonate group together with some weak bands characteristic of Pr-oxide at 398 and 570 cm^{-1} [4, 19, 31]. To support these results, in Fig. 7 the spectrum of the product decomposition of Pr-carbonate octahydrate treated at 450°C is also shown. Both compounds present very similar spectra. A substantial part of the complex and of the carbonate, respectively, has been converted to the unidentate carbonate intermediate and it is shown by the shifts in both asymmetrical and symmetrical stretching frequencies. According to XRD data, the process at 450°C involves decomposition of the carbonate to give $Pr_2O_2CO_3$ (JCPDS No. 25-696) as a major phase. In the DTA/TG curves the process is exothermic and brings the total mass loss to 44.57% from the total mass loss of 90.03% and involves the Pr-CA complex decomposition into $Pr_2O_2CO_3$ (JCPDS No. 25-696). Few traces of $PrO_{1.83}$ were also detected according to XRD data, but the product was not well crystallized. In IR spectra at 450°C new absorption bands can be seen displayed at 840, 855, 878, 1370, 1455, 1507 cm^{-1} assignable to the vibrations modes of unidentate carbonate group [19, 32]; the additional bands appearing in the 850 cm^{-1} are the bands in the out-of-plane bending region. In the spectra of the specimen treated at 450°C in oxygen, a weak band characteristic of Pr-oxide bond formation could be detected at 512 cm^{-1}. In this spectrum, distinct absorptions are seen in the region of carboxyl and carbonate stretching, but the results of XRD showed a quite amorphous compound. For the specimen treated in nitrogen the IR spectra displayed the characteristic bands of carbonate species due to the presence of $Pr_2O_2CO_3$ (JCPDS No. 25-696) and some weak bands of Pr-oxide at 390, 400 and 421 cm^{-1}. However, the XRD identification for the compound treated in nitrogen at 450°C was not very useful because the product was amorphous. IR spectra of the products obtained at 1000°C display bands due to praseodymium oxide. The absorption intensities of the specimens treated at 1000°C became smaller than those of the samples treated at 450°C. Bands due to carbonate species are present as minor features or disappeared completely. The spectra of the oxides appear especially in the 600–250 cm^{-1} region [4, 19]. Pr-oxide bands appeared in the IR spectra of the treated citrate, in accordance with the XRD patterns and literature data [4, 5, 19, 33]. In the spectra of the specimens treated at 1000°C in air and oxygen, bands due to the Pr-oxide could be detected at 380, 395 and 600 and 428, 463, 512 and 588 cm^{-1}, respectively. IR spectrum of the calcination products at 1000°C in nitrogen displays weak bands at 380 and 389 cm^{-1}. XRD of the product shows it is predominantly amorphous and only one band of $Pr_2O_2CO_3$ could be detected. Even the bands of Pr-oxide are weak in some regions, the decomposition of the oxycarbonate is taking place from the non-appearance of the degenerate in plane bending mode. A major difference in the DTA curves in air compared to those in N_2 was observed for the complex. DTA in air was characterized by a very sharp or strong exothermic effect at the initial stage of decomposition while in the case of using nitrogen atmosphere, a very broad exothermic effect could be noticed on the DTA curve. The different thermal decomposition behaviour of the citrate complex in air and nitrogen affects the change in the oxidation state of the Pr ion from Pr(III) in the Pr-CA gel and in the oxycarbonate to a higher valence in the final oxide $PrO_{1.83}$. The kinetics of the decomposition reaction in air and oxygen is faster than in nitrogen. Nitrogen atmosphere inhibits the decomposition of the Pr citrate complex as XRD results also confirm, observation which agrees with other data reported in literature for the thermal reactions of other similar lanthanide complexes [11].

Based on DTA/TG, XRD and IR analyses, the reactions during the thermal decomposition of the Pr-CA complex are summarized in Table 1, together with the temperature ranges over which they occurred, according to the mass losses observed in TG measurements.

Table 1 Attribution of thermal effects, experimental mass loss of the Pr-CA complex treated in different atmospheres

Temperature range/°C	Thermal effects		Mass loss/ % experimental	Final products of the left-overs according to XRD data
	endo	exo		
			Pr-CA complex in air	
20–242	–	–		
242–390	–	330 sh*	90.03	
390–1000	–	410 420 sh*		$PrO_{1.83}$
			Pr-CA complex in N_2	
20–322	–	broad	67.40	$Pr_2O_2CO_3$
322–1000	–	910		
			Pr-CA complex in O_2	
20–340	–	300	96.55	$PrO_{1.83}$
340–1000	–	390		

*shoulder

By decomposition of both Pr carbonate used as raw material in our synthesis and Pr-CA complex, a PrO_x (x=1.83) phase with perovskite cubic structure was formed as final decomposition product. As previously mentioned, PrO_x comprises different stoichiometries and structures, therefore a careful XRD identification of the X-ray reflections of our final product at intermediate and final temperatures was necessary, in order to verify all the possible oxide modifications from JCPDS data base. Shifting of the peaks from our decomposition oxides correspond to the $PrO_{1.83}$ cubic structure (JCPDS 6-329) also reported as the Pr_6O_{11} in (JCPDS 41-1219) with the space group Fm3m, taking into account that other Pr-oxides did not match the final oxide formation by the decomposition Pr-CA complex or of the Pr-carbonate used in our synthesis; this fact is also confirmed by the lattice parameter results, calculated from the X-ray diffraction pattern of the final oxide obtained by the Pr-CA complex decomposition. The lattice parameters reported in literature (JCPDS 24-1006, 42-1121, 6-329) and our experimental value are shown in Fig. 8. The average value of 1.82 of the oxy-

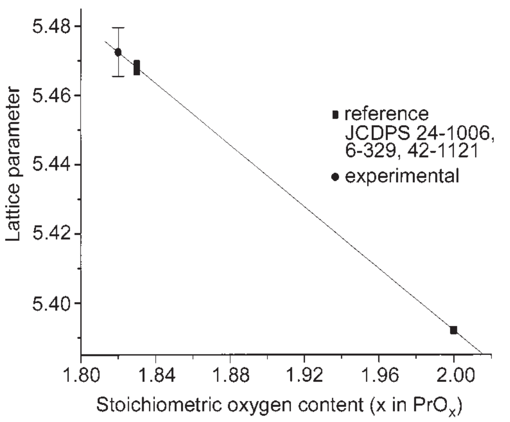

Fig. 8 Lattice parameter for the cubic structure *vs*. the stoichiometric oxygen content (x in PrO_x), compared with the value for the oxide obtained after thermal decomposition of Pr-CA complex

gen content in the final oxide obtained by the Pr-CA decomposition has been determined by linear fitting on literature data. This value reflects that the stoichiometry of the final oxide is very close to the reported data of 1.83 in the XRD patterns, which is actually within the experimental error. Therefore, it is not possible to determine precisely if there is a real oxygen deficiency from a stoichiometric $PrO_{1.83}$ value.

The results permit suggestions concerning the composition and mechanism of thermal decomposition of Pr-CA complex and the reactions can be summarized as follows:

In air

$$\text{Pr-CA complex} \xrightarrow{450^\circ C} Pr_2O_2CO_3 + PrO_{1.83} \xrightarrow{1000^\circ C} PrO_{1.83}$$

In oxygen:

$$\text{Pr-CA complex} \xrightarrow{450^\circ C} PrO_{1.83} \xrightarrow{1000^\circ C} PrO_{1.83}$$

In nitrogen:

$$\text{Pr-CA complex} \xrightarrow{450^\circ C} \text{amorphous} \xrightarrow{1000^\circ C} Pr_2O_2CO_3$$

Pr-CA complex on heating decomposes to $PrO_{1.83}$ with formation of intermediate $Pr_2O_2CO_3$ in air or directly to the oxide in flowing oxygen. In nitrogen atmosphere, amorphous products were obtained after thermal decomposition, however traces of oxycarbonate $Pr_2O_2CO_3$ were detected at 1000°C.

Conclusions

The amorphous citrate method was used to synthesize the Pr-CA complex, starting form Pr-carbonate octahydrate dissolved in water and citric acid. The Pr-CA complex decomposes in air similar to $Pr_2(CO_3)_3 \cdot 8H_2O$, with formation of $Pr_2O_2CO_3$ as intermediate and of the oxide $PrO_{1.83}$ as final product. The decomposition of the complex was influenced by the ambient atmosphere. The XRD, IR and DTA/TG/DTG results showed that Pr-CA dehydrates and decomposes up to 450°C with formation of the intermediate $Pr_2O_2CO_3$ or directly to $PrO_{1.83}$ depending on the composition of the gas atmosphere. $PrO_{1.83}$ was formed at 450°C in the case of the thermal decomposition of Pr-CA complex in flowing oxygen, while in the case of air $Pr_2O_2CO_3$ was detected as major phase. The thermoanalytical study was useful to detect the formation of the intermediates and to determine the influence of the atmosphere on the final decomposition products.

References

1 Handbook on the Physics and Chemistry of Rare Earths, Ed. by K. A. Gschneidner Jr. and L. Eyring, Vol. 3, North Holland Publ., Amsterdam 1979.
2 K. Muraishi, K. Nagase, M. Kikuchi, K. Sone and N. Tanaka, Bull. Chem. Soc. Jpn., 55 (1982) 1845.
3 E. R. Birnbaum, Gmelin Handbook of Inorganic Chemistry, 8th ed., System No. 39, Part D5, Springer, Berlin 1984, p. 1.
4 G. A. M. Hussein, J. Anal. Appl. Pyrolysis, 29 (1994) 89.
5 G. A. M. Hussein, J. Anal. Appl. Pyrolysis, 37 (1996) 111.
6 K. Otsuka, Inorg. Chim. Acta, L31 (1986) 115.
7 A. Cotton and G. Wilkinson, Advanced Inorganic Chemistry 5th Ed., Wiley, New York 1988, p. 976.
8 S. S. Moosath, J. Abraham and T. W. Swaminathan, Z. Anorg. Chem., 324 (1963) 90.
9 G. A. M. Hussein, J. Chem. Soc., Faraday Trans., 91 (1994) 1385.
10 A. Glasner and M. Steinberg, J. Inorg. Nucl. Chem., 16 (1961) 279; 22 (1961) 39.
11 K. Muraishi, H. Yokobayashi and K. Nagase, Thermochim. Acta, 182 (1991) 209.
12 W. Brzyska and B. Paszkowska, J. Therm. Anal. Cal., 51 (1998) 561.
13 W. Brzyska and A. Krol, Thermochim. Acta, 182 (1991) 293.
14 W. Brzyska and A. Kula, J. Therm. Anal. Cal., 53 (1998) 161.
15 M. Kakihana, J. Sol–Gel Sci. Technol., 6 (1996) 7.
16 M. Kakihana, S. Kato, V. Petrykin, J. Backström, L. Börjesson and M. Osada, Phys. C, 312 (1999) 74.
17 M. Popa and M. Kakihana, Solid State Ionics, in press.
18 M. Kakihana and M. Yoshimura, Bull. Chem. Soc. Jap., 72 (1999) 1427.
19 J. A. Goldsmitch and S. D. Ross, Spectrochim. Acta, 23A (1967) 1909.
20 A. F. Clifford and P. A. Faeth, Rare Earth Research III, Gordon & Breach, 1963, p. 36.
21 R. L. N. Sastry, S. R. Yogonarasimhan, P. L. Mehrota and C. N. R. Rao, J. Inorg. Nucl. Chem., 28 (1966) 1165.
22 R. C. Vickery, Chemistry of the Lanthanons, Academic Press, 1953.
23 E. L. Head and C. E. Holley Jr., Rare Earth Research II, Gordon & Breach, 1963, p. 51.
24 P. Caro and J. Loriers, J. Rech. Centre Natl. Rech. Sci., 39 (1957) 107.
25 G. Pannentier, J. Natal and A. Dereigne, Bull. Soc. Chem. France, 12 (1965) 318.
26 P. Caro, Compt. Rend., 262C (1966) 992.

27 L. Moscardini D'Assuncao, I. Giolito and M. Ionashiro, Thermochim. Acta, 137 (1989) 319.
28 R. C. Paul, M. S. Bains and J. S. Ghotra, Indian J. Chem., 7 (1969) 214.
29 M. W. Porter and R. C. Spiller, Barker Index of Crystals, Vol. 1, part 2, refs 0378/9, W. Heffer, 1951.
30 L. J. Bellamy, The infrared spectra of complex molecules, Chapman and Hall, London 1975, p. 176.
31 P. Tarakeshwar and S. Manogran, Spectrochim. Acta, 50A (1994) 2327.
32 K. Nakamoto, Infrared and Raman Spectra of Inorganic and Coordination Compounds, Part A 5th Ed. Wiley, New York 1997.
33 G. A. M. Hussein, Thermochim. Acta, 186 (1991) 187.